

Supporting Information

**Targeting the tumor core: hypoxia-responsive
nanoparticles for delivery of chemotherapy to
pancreatic tumors**

*Matthew I. Confeld¹, Babak Mamnoon¹, Li Feng¹, Heather Jensen-Smith², Priyanka Ray³, Jamie
Froberg⁴, Jiha Kim⁵, Michael A. Hollingsworth², Mohiuddin Quadir³, Yongki Choi⁴, Sanku
Mallik¹ **

¹North Dakota State University, Pharmaceutical Sciences, Fargo, North Dakota, USA

²Fred & Pamela Buffett Cancer Center, Eppley Institute for Research in Cancer, University of
Nebraska Medical Center, Omaha, Nebraska, USA

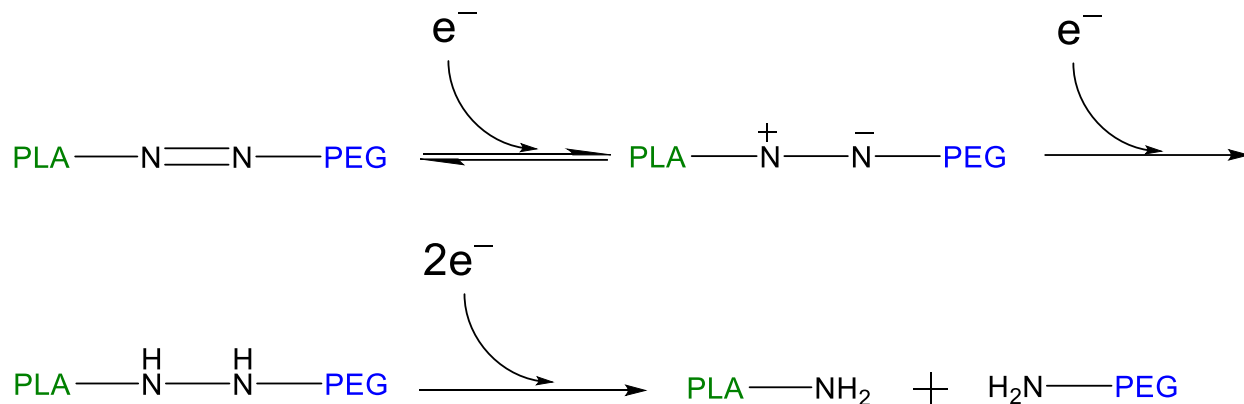
³North Dakota State University, Coatings and Polymeric Materials Department, Fargo, North
Dakota, USA

⁴North Dakota State University, Physics Department, Fargo, North Dakota, USA

⁵North Dakota State University, Department of Biological Sciences, Fargo, North Dakota, USA

Table of Contents

Scheme S1. Proposed mechanism of azobenzene reduction under hypoxia.	3
Table S1. Polymersome characterization (size and polydispersity index by dynamic light scattering).....	3
Figure S1. Critical Aggregation Concentration (CAC) of the polymer PLA ₆₀₀₀ –diazobenzene–PEG ₂₀₀₀	4
Figure S2. Infrared spectrum of PLA ₆₀₀₀ –diazobenzene–PEG ₂₀₀₀	5
Figure S3. ¹ H NMR spectrum (CDCl ₃) of the hypoxia-responsive polymer PLA ₆₀₀₀ –diazobenzene–PEG ₂₀₀₀	6
Figure S4. ¹³ C NMR (CDCl ₃) of the hypoxia-responsive polymer PLA ₆₀₀₀ –diazobenzene–PEG ₂₀₀₀	7
.....	7
Figure S5. GPC in THF of the hypoxia-responsive polymer PLA ₆₀₀₀ –diazobenzene–PEG ₂₀₀₀	8
Figure S6. MALDI-TOF mass spectrum of the synthesized iRGD peptide.	9
Figure S7. Circular dichroism (CD) spectrum of the synthesized iRGD peptide.....	9
Figure S8. Polymersome stability in human serum.	10
Figure S9. Size of the polymersomes (by dynamic light scattering) of the polymersomes as a function of time in hypoxia and normoxia.....	10
Figure S10. Penetration of ICG Encapsulated polymersomes in mice orthotopic pancreatic tumors	11
Figure S11. Accumulation of polymersomes in various organs.	12
Figure S12: Changes in mouse weights during treatments with polymersomes encapsulated drugs.	13
Figure S13: Changes in mouse weights during treatments with the free drugs.....	14



Scheme S1. Proposed mechanism of azobenzene reduction under hypoxia.

Sample Name	Size (nm)	Poly Dispersity Index	Zeta-Potential (mV)	Entrapment Efficiency (%)	Loading Content (%)
iPsome (buffer only)	107 ± 2	0.11	-3.2 ± 0.4	n/a	n/a
Gemcitabine iPsome (iGem)	117 ± 2	0.14	-10.3 ± 0.5	63% ± 5	13.8 ± 2.2
Napabucasin iPsome (iNap)	188 ± 6	0.3	0.1 ± 0.4	34% ± 4	21.3 ± 3.3

Entrapment Efficiency Equation

$$\frac{\text{amount of drug added} - \text{amount of drug encapsulated}}{\text{amount of drug added}} \times 100$$

Loading Content Equation

$$\frac{\text{total weight of drug loaded in polymersomes}}{\text{total weight of polymer}} \times 100$$

Table S1. Polymersome characterization (size and polydispersity index by dynamic light scattering). The size and polydispersity index were measured using dynamic light scattering and by averaging the results of three measurements done with ten different runs of the sample and using at least three different batches of the synthesized polymersomes.

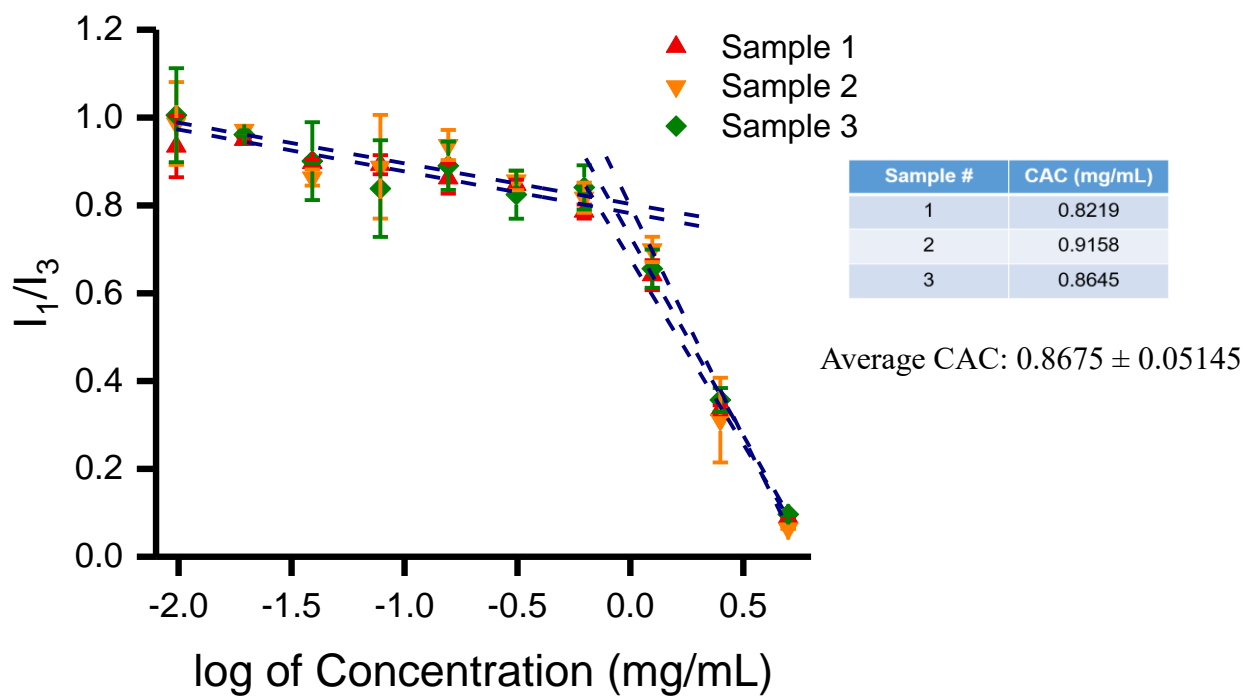


Figure S1. Critical Aggregation Concentration (CAC) of the polymer PLA₆₀₀₀–diazobenzene–PEG₂₀₀₀. The average CAC was measured using 3 samples and value of 0.8675 ± 0.05145 mg/mL was calculated.

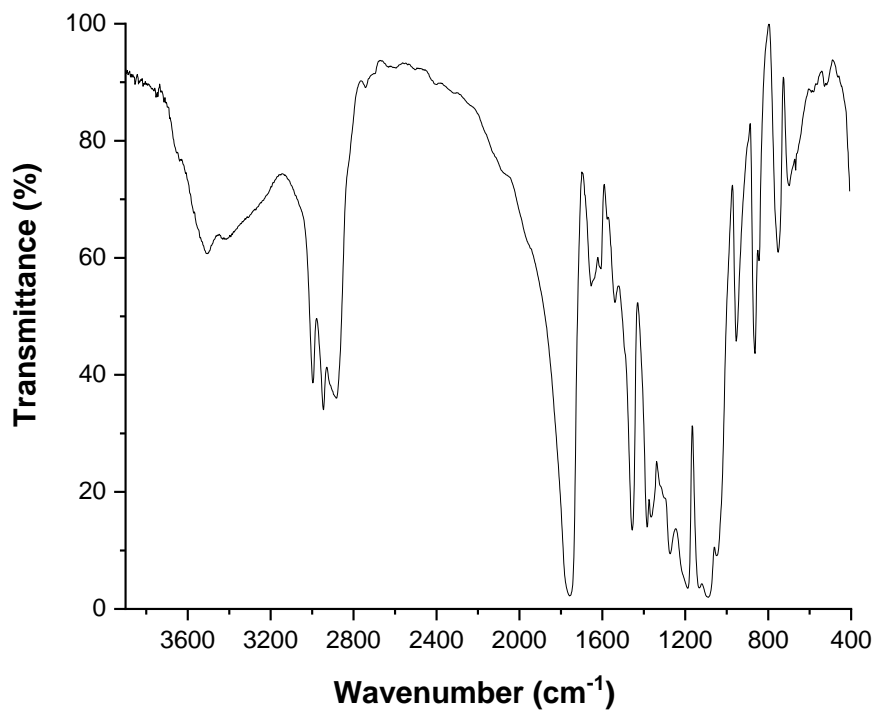


Figure S2. Infrared spectrum of PLA₆₀₀₀-diazobenzene-PEG₂₀₀₀. Fourier transform infrared spectroscopy (FTIR) was performed using a Thermo Scientific Nicolet 8700 FTIR instrument. The sample was mixed with KBr powder and pressed to form a KBr pellet under pressure. The sample was scanned 32 times. Spectrum was recorded were in the range of 4000 - 400 cm⁻¹ at a spectral resolution of 4 cm⁻¹.

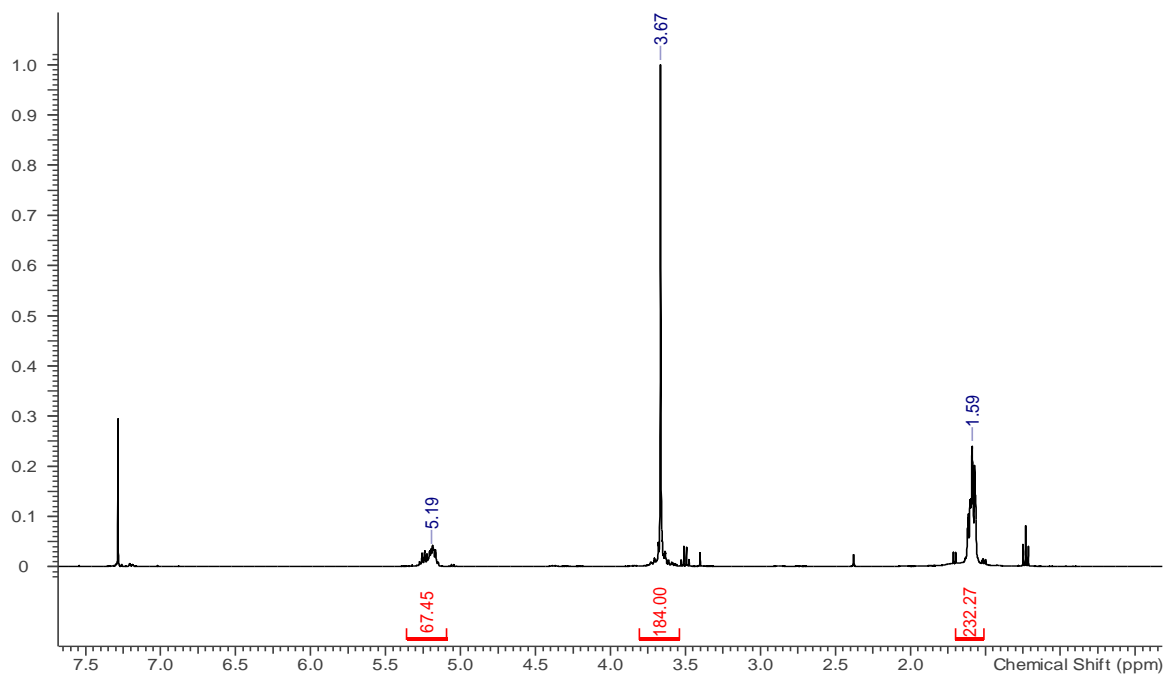
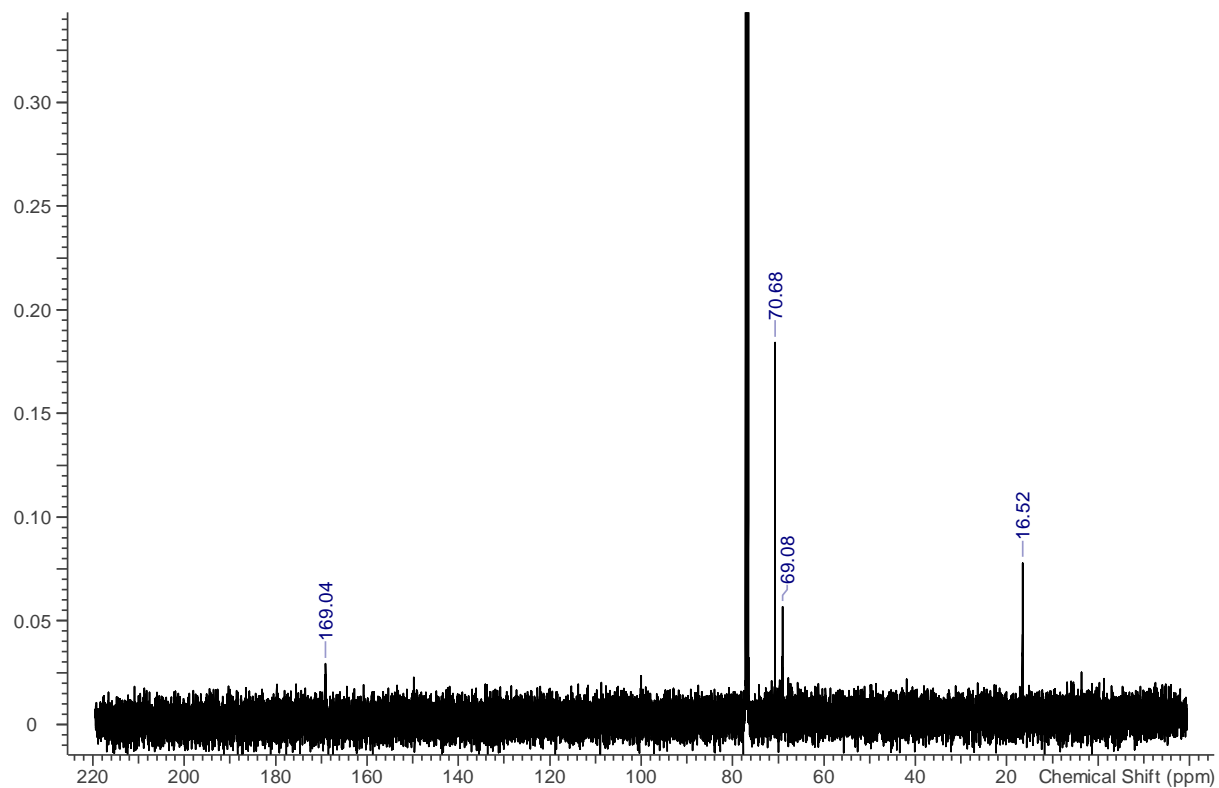
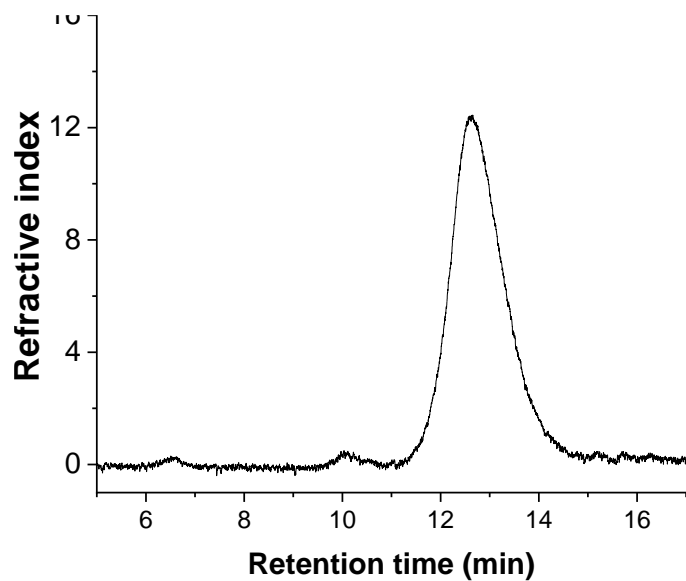


Figure S3. ^1H NMR spectrum (CDCl₃) of the hypoxia-responsive polymer PLA₆₀₀₀-diazobenzene-PEG₂₀₀₀.



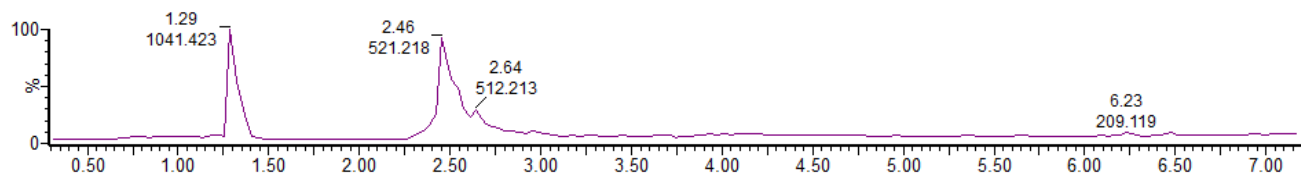
169.04 ($(-\text{CH}-\text{C}=\text{O})$), 69.08 ($(-\text{CH}-\text{C}=\text{O})$), 70.68 ($(\text{CH}_2-\text{CH}_2-\text{O})$), 16.52 ($(\text{CH}_3-\text{CH}-\text{C}=\text{O})$)

Figure S4. ^{13}C NMR (CDCl_3) of the hypoxia-responsive polymer PLA_{6000} -diazobenzene- PEG_{2000} .



Mn	5,580	Mw	6,451
Mz	7,391	Mz+1	8,459
Mv	6,451	Mp	6,535
Mz/Mw	1.147	Mw/Mn (PDI)	1.156

Figure S5. GPC in THF of the hypoxia-responsive polymer PLA₆₀₀₀-diazobenzene-PEG₂₀₀₀.



RT=2.46, base peak 521.218 is a double charged 1041.423

Figure S6. MALDI-TOF mass spectrum of the synthesized iRGD peptide.

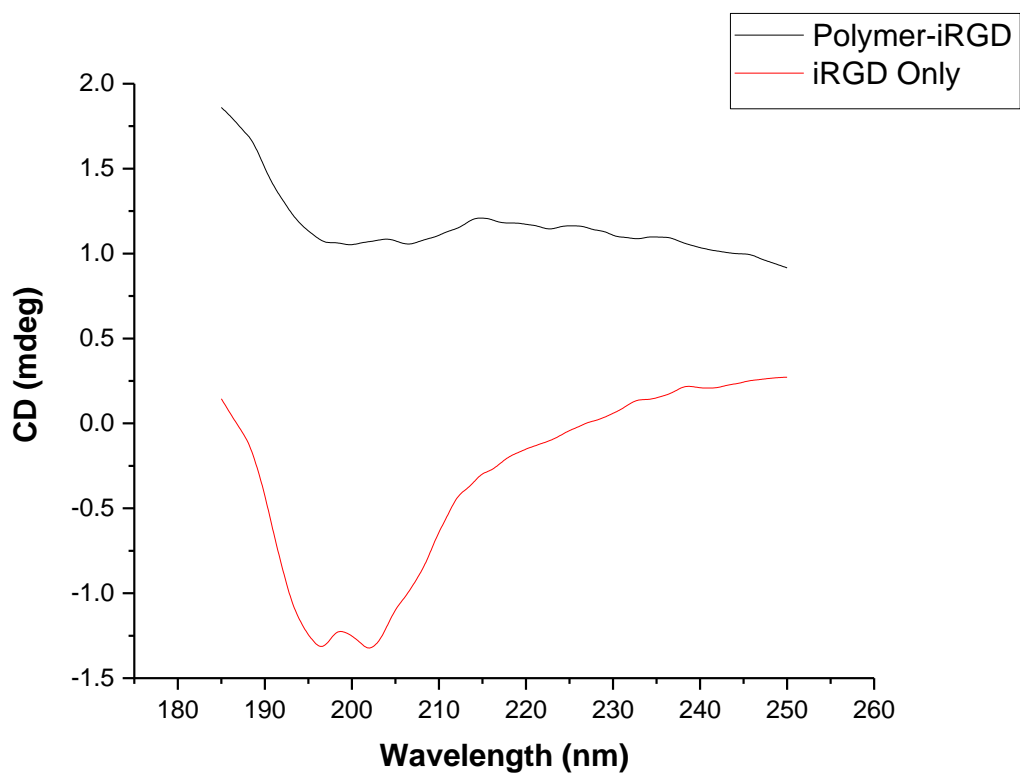


Figure S7. Circular dichroism (CD) spectrum of the synthesized iRGD peptide.

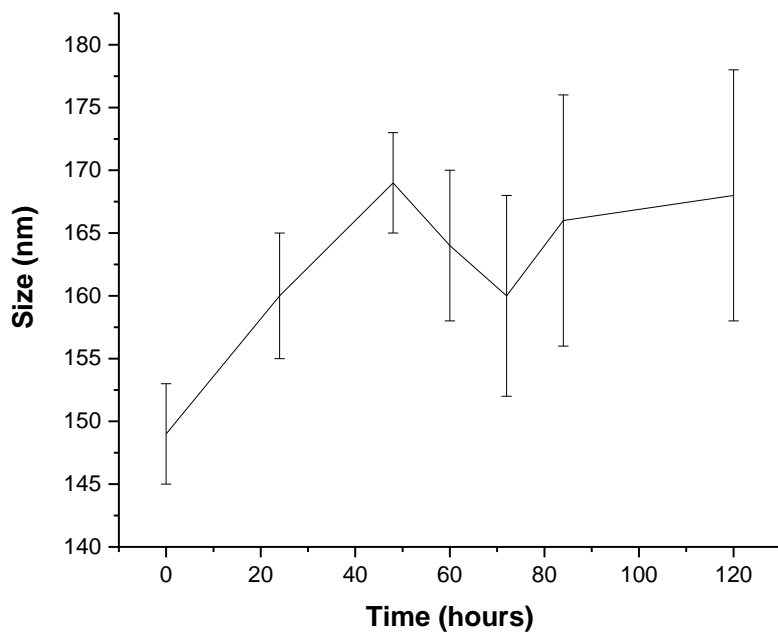


Figure S8. Polymersome stability in human serum. The initial size was 149 (± 4) nm and after 120 hours the average size was 168 (± 5) nm. N = 3.

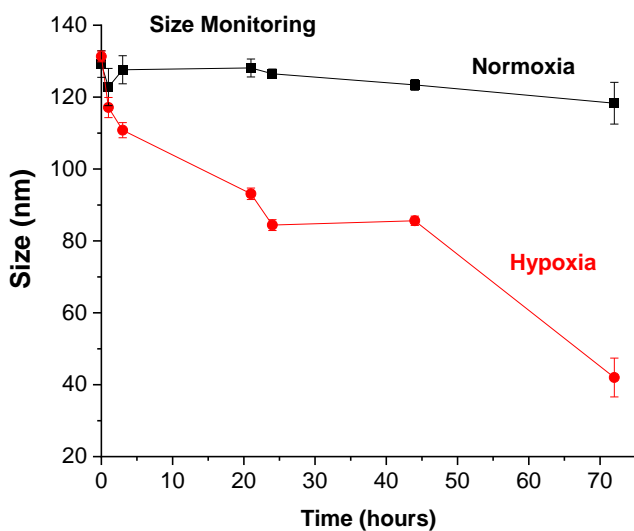


Figure S9. Size of the polymersomes (by dynamic light scattering) of the polymersomes as a function of time in hypoxia and normoxia.

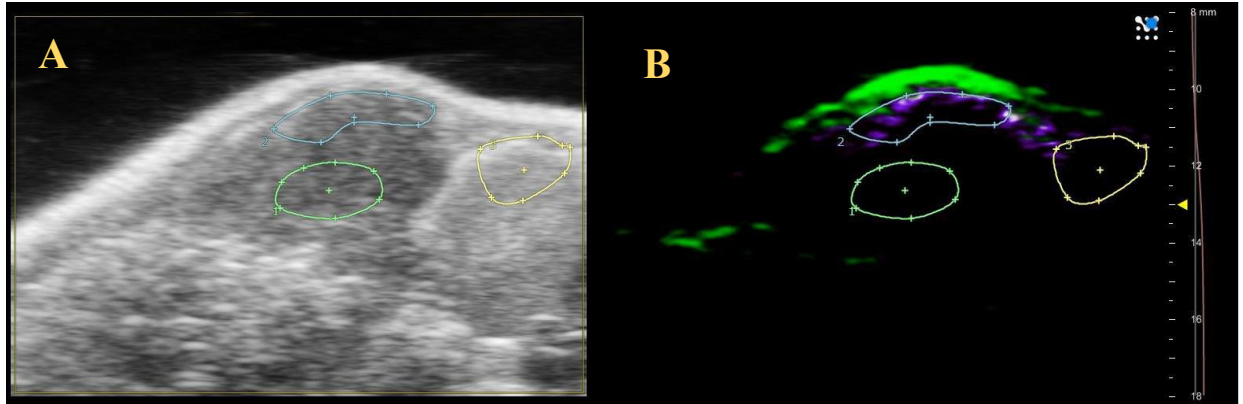


Figure S10. Penetration of ICG Encapsulated polymersomes in mice orthotopic pancreatic tumors. **(A)** Ultrasound image of orthotopic PDAC tumor. The blue selection indicates tumor edge, yellow is the unaffected normal pancreas, and light green represents the tumor core. **(B)** Photoacoustic image of released ICG (green) and encapsulated ICG (purple) at 1-hour post tail vein injection.

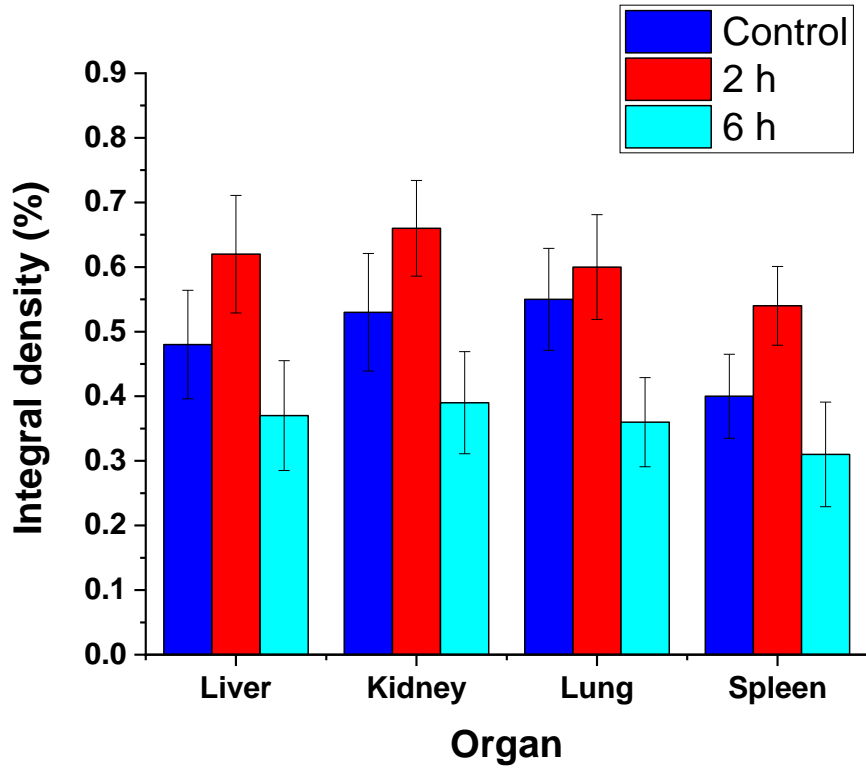


Figure S11. Accumulation of polymersomes in various organs. Mice organs were collected at 2 hours and 6 hours post-injection of lissamine rhodamine dye containing polymersomes. NIH ImageJ software was used to quantify fluorescent intensity of organs (n = 3).

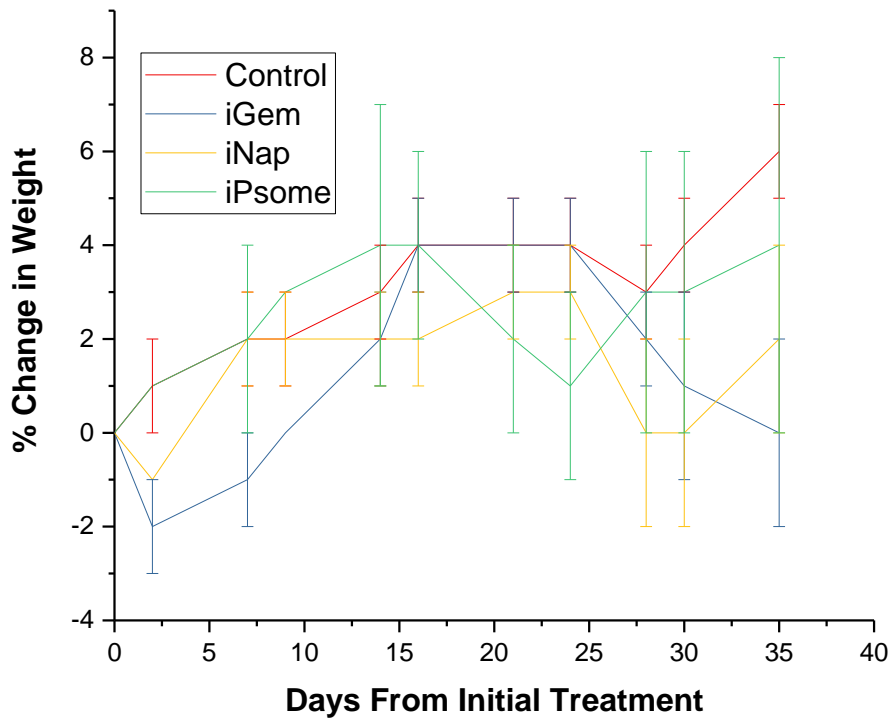


Figure S12: Changes in mouse weights during treatments with polymersomes encapsulated drugs.

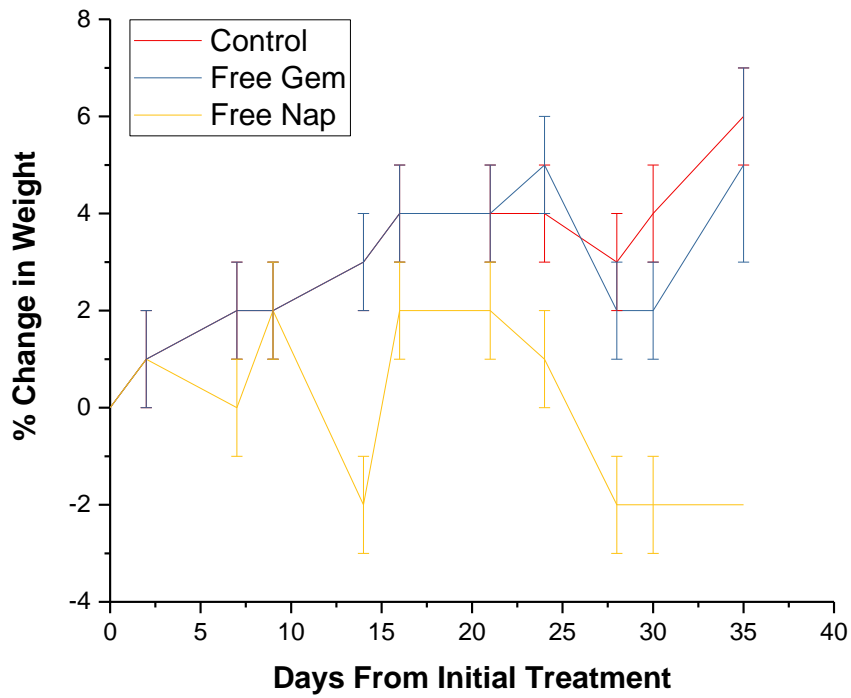


Figure S13: Changes in mouse weights during treatments with the free drugs.

In-Vivo Tumor Volumes Data
Excel File